Supplementary Information for: Decamethylruthenocene Hydride and Hydrogen Formation at Liquid|Liquid Interfaces

Lucie Rivier,[a] T. Jane Stockmann,[a,b] Manuel A. Méndez,[a] Micheál D. Scanlon,[a,c] Pekka Peljo,[a] Marcin Opallo,[d] and Hubert H. Girault[a,†]

[a] Laboratoire d'Electrochimie Physique et Analytique, Ecole Polytechnique Fédérale de Lausanne (EPFL), Rue de l'Industrie 17, CH-1951 Sion, Switzerland.

[b] Sorbonne Paris Cité, Paris Diderot University, Interfaces, Traitements, Organisation et Dynamique des Systèmes, CNRS-UMR 7086, 15 rue J. -A. Baïf, 75013 Paris - France.

[c] Department of Chemistry, the Tyndall National Institute and the Analytical & Biological Chemistry Research Facility (ABCRF), University College Cork, Cork, Ireland.

[d] Institute of Physical Chemistry, Polish Academy of Sciences, ul. Kasprzaka 44/52, 01-224 Warszawa, Poland.

[†] To whom correspondence should be addressed. Tel: +41-21-693 3145; Fax: +41-21-693 3667

Email: hubert.girault@epfl.ch; URL: http://lepa.epfl.ch/

Table of Contents:

Additional Electrolytic Cells:

$$\mathrm{Ag}\left|\mathrm{AgCl}\right|\begin{matrix}\text{10 mM LiCl}\\\text{1 mM BACl}\\\text{(w~ref.)}\end{matrix}\left|\begin{matrix}\text{5 mM } \mathrm{Cp^*_2Ru^{(II)}}\\\text{5 mM BATB}\\\text{(DCE)}\end{matrix}\right\|\begin{matrix}\text{0.5 mM } \mathrm{H_2SO_4}\\\text{(w)}\end{matrix}\left|\mathrm{Ag_2SO_4}\right|\mathrm{Ag} \qquad \text{Cell S1}$$

$$\mathrm{Ag}\left|\mathrm{AgCl}\right|\begin{matrix}\text{10 mM LiCl}\\\text{1 mM BACl}\\\text{(w~ref.)}\end{matrix}\left|\begin{matrix}\text{5 mM } \mathrm{Cp^*_2Ru^{(II)}}\\\text{5 mM BATB}\\\text{(DCE)}\end{matrix}\right\|\begin{matrix}\text{5 mM } \mathrm{Li_2SO_4}\\z\text{ M KCl}\\\text{(w)}\end{matrix}\left|\mathrm{Ag_2SO_4}\right|\mathrm{Ag} \qquad \text{Cell S2}$$

$$\mathrm{Ag}\left|\mathrm{AgCl}\right|\begin{matrix}\text{10 mM LiCl}\\\text{1 mM BACl}\\\text{(w~ref.)}\end{matrix}\left|\begin{matrix}\text{4 mM } \left[\mathrm{Cp^*_2Ru^{(III)}}\right]^+\\\text{20 mM BATB}\\\text{(DCE)}\end{matrix}\right\|\begin{matrix}\text{0.005 M } \mathrm{H_2SO_4}\\\text{(w)}\end{matrix}\left|\mathrm{Ag_2SO_4}\right|\mathrm{Ag} \qquad \text{Cell S3}$$

$$\mathrm{Ag}\left|\mathrm{AgCl}\right|\begin{matrix}\text{10 mM LiCl}\\\text{1 mM BACl}\\\text{(w~ref.)}\end{matrix}\left|\begin{matrix}z\text{ μM } \mathrm{Cp^*_2Ru^{(II)}}\text{+125 μM HTB}\\\text{5 mM BATB}\\\text{(DCE)}\end{matrix}\right\|\begin{matrix}\text{0.01 mM HCl}\\\text{(w)}\end{matrix}\left|\mathrm{AgCl}\right|\mathrm{Ag} \qquad \text{Cell S4}$$

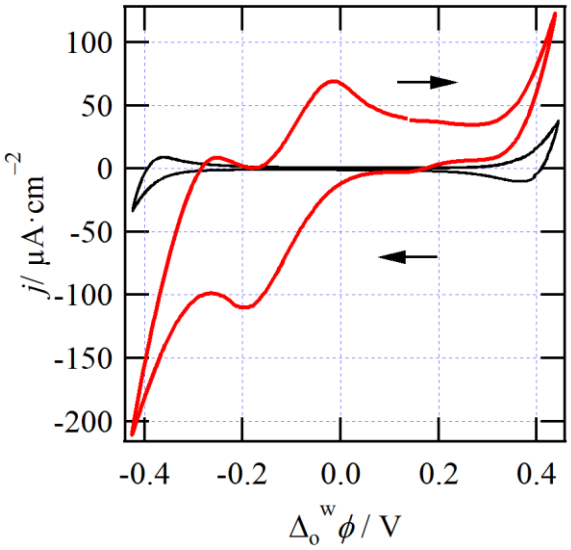

Figure S1: Experimental cyclic voltammograms recorded using Cell S1 with (red trace) and without (black trace) $\left[\mathrm{Cp^*_2Ru^{(III)}}\right]^+$ dissolved in the DCE phase. All other instrument parameters were the same as in Figure 1.

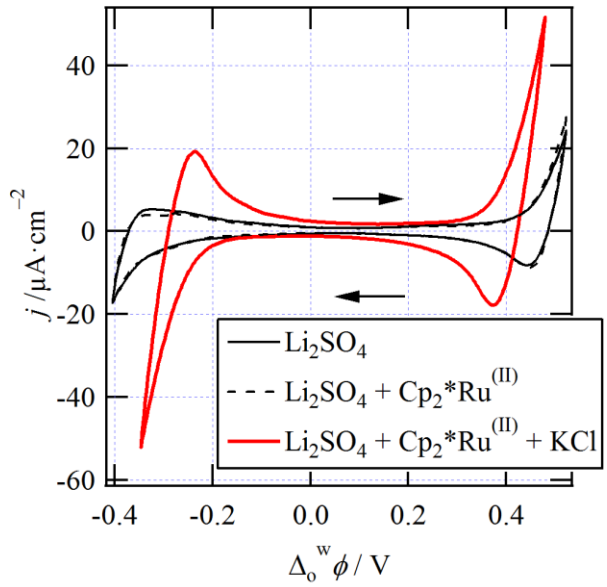

Figure S2: Experimental cyclic voltammograms recorded using Cell S2 with a drop of a solution of 0.5 M KCl added to the aqueous phase (red trace), without KCl (black trace) and without KCl and $Cp_2^*Ru^{(II)}$ (dashed curve). All other conditions were the same as in Figure S1.

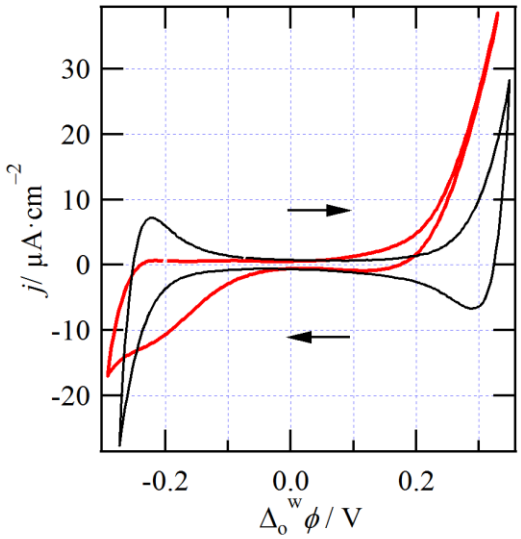

Figure S3: Cyclic voltammograms obtained using Cell S3 with (red trace) and without (black trace) $Cp_2^*Ru^{(II)}$ dissolved in the DCE phase, along with 5 mM of H_2SO_4 in the aqueous phase. All other conditions were the same as in Figure S1.

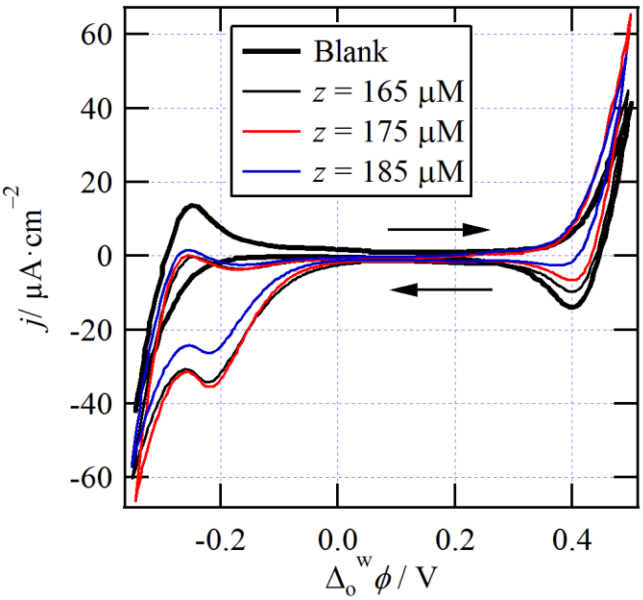

Figure S4: Cyclic voltammograms obtained using Cell S4 and varying *z* as indicated while the blank curve (▬) was acquired in the absence of HTB and $Cp^*_2Ru^{(II)}$.

Preparation of tetrakis(pentafluorophenyl)borate diethyl acid (HTB).

2 g of $[Li(OEt_2)_2]TB$ was dissolved in 30 mL of 6 M HCl (Acros) to prepare HTB. Next, $[H(OEt_2)_2]TB$ was extracted by addition of DCM (30 mL) and the aqueous layer was further washed with DCM (2 × 15 mL) after phase separation. The combined organic layers were dried over sodium sulfate (Na_2SO_4, Reactolab). Finally, Na_2SO_4 was removed by filtration and DCM evaporated under reduced pressure to yield the organic soluble acid $[H(OEt_2)_2]TB$ as a white powder.

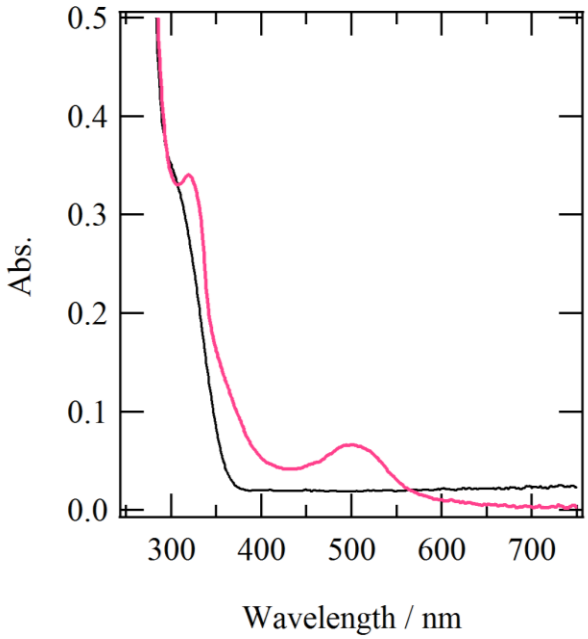

Figure S5: UV/Vis absorbance spectra obtained using Vial 1 after first preparing the solution (black trace) and after stirring for 60 min under illumination (pink trace).

Simulation Details

Herein, Fick's laws were used to describe diffusion of the various chemical species; for example, species *i* of concentration c_i with a diffusion coefficient D_i through the following relation:

$$\frac{\partial c_{i,w}(x,t)}{\partial t} = D_{i,w}\nabla c_{i,w}(x) = D_{i,w}\frac{\partial c_{i,w}(x)}{\partial x} \quad (1)$$

Equation (1) has been written for an ion dissolved in the aqueous phase (w); however, an equivalent equation can be for the 1,2-dichloroethane (DCE) or organic phase (o). The electrochemical flux of ions across the ITIES was simulated using the Butler-Volmer kinetic equations in the form of (2) and (3), below:

$$k_f = k^0 \exp\left[-\alpha f(\Delta_o^w\phi - \Delta_o^w\phi^{o'})\right] \quad (2)$$

$$k_b = k^0 \exp\left[(1-\alpha) f(\Delta_o^w\phi - \Delta_o^w\phi^{o'})\right] \quad (3)$$

Such that k^o, α, and $\Delta_o^w\phi^{o'}$ represent the standard rate constant, the transfer coefficient, and the formal ion transfer potential, respectively. $\Delta_o^w\phi$ is the Galvani potential difference across the interface; while experimentally this is controlled externally through a potentiostat, it was replicated in the simulation through application of a triangular waveform. Ultimately, k_f and k_b represent the electrochemical rate of simple ion transfer as shown in equation (4):

$$i_w^z \underset{k_b}{\overset{k_f}{\rightleftharpoons}} i_o^z \quad (4)$$

Finally, the current was related to the overall flux of ions across the interface through equation (5):

$$J(x,t) = FA\sum_i z_i D_{i,w} \nabla c_{i,w}(x,t) \quad (5)$$

Where the electrode area, A, was chosen so as to be reflective of the experimental and defined by a circle of radius 0.7 cm. The simulation mesh was validated using simple IT and comparison of the peak current to the Randles-Sevčik equation[1,2] as demonstrated recently. [3]
A list of the parameters and coefficients employed have been provided in Table S1.

Table S1: List of the terms and coefficients employed in the simulations.

Term	Initial Values	Description
$c^*_{H^+,aq}$	1, 10, 100, and 1000 mM	Initial aqueous proton concentration
$c^*_{DMRc,org}$	5 mM	Initial organic phase DMRc concentration
$D_{H^+,aq}$	9.4×10^{-5} cm^2·s^{-1}	Aqueous proton diffusion coefficient
$D_{H^+,org}$	1×10^{-5} cm^2·s^{-1}	H^+ diffusion coefficient in the organic phase
$D_{DMRc,org} = D_{DMRc,aq}$	7.26×10^{-6} cm^2·s^{-1}	Diffusion coefficient of DMRc[†]
k_{cf1}	1×10^5 L·mol^{-1}·s^{-1}	Rate of hydride formation in the organic phase
k_{cb1}	1 s^{-1}	Rate of hydride dissociation in the organic phase
k_{cf2}	1 L·mol^{-1}·s^{-1}	Rate of hydride formation in the aqeuous phase
k_{cb2}	1×10^5 s^{-1}	Rate of hydride dissociation in the aqueous phase
k_{pf}	1×10^{-6} cm·s^{-1}	Rate of DMRc (neutral) from the aqueous to organic phase
k_{pb}	1×10^{-10} cm·s^{-1}	Rate of DMRc (neutral) from the organic to aqueous phase
v	0.050 V·s^{-1}	Scan rate

[†]These were used to describe $\left[Cp^*_2 Ru^{(IV)} H^+ \right]$ in either phase.

EC′ mechanism

A two-step mechanism involving a potential dependent ion transfer step (eq. S1, electrochemical step) followed by a bulk, organic phase homogeneous reaction (eq. S2), as provided below:

$$i^z_w \rightleftharpoons i^z_o \quad [S1]$$

$$i^z_o + L_o \xrightarrow{k_1} iL^z_o \quad [S2]$$

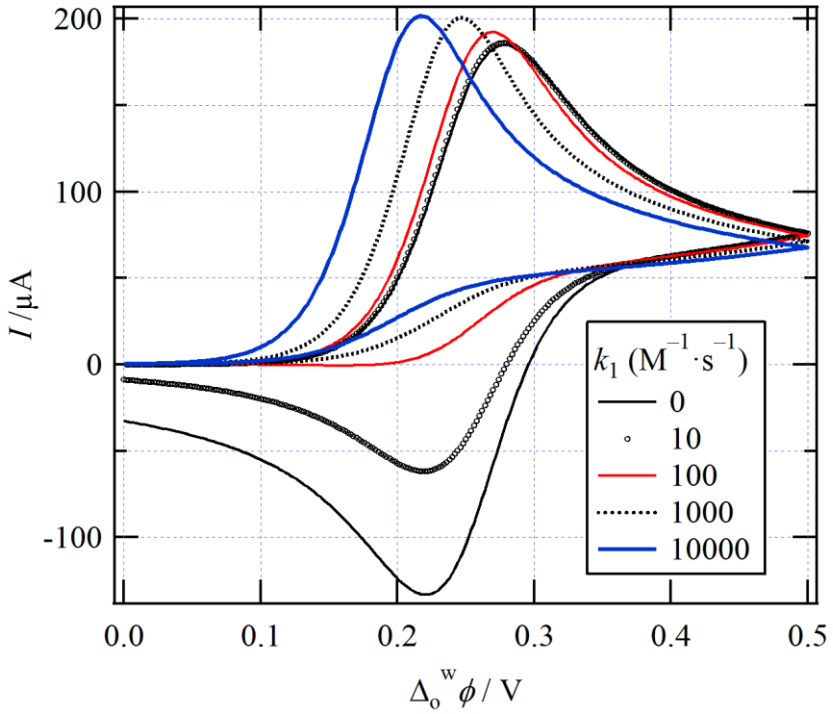

Figure S6: Simulated cyclic voltammograms generated using the EC′ mechanism (eq. S1 and S2, above); here, the rate, k_1, of the complexation step has been altered as indicated inset. The formal ion transfer potential of i^z was 0.250 V, with $D_{i,w} = D_{i,o} = 1 \times 10^{-5}$ cm^2·s^{-1}, $c_{i,w} = 1$ mmol·L^{-1}, $c_{i,o} = 0$ mmol·L^{-1}, $L_o = 5$ mmol·L^{-1}, and $v = 0.020$ V·s^{-1}.

Complete author list:

(13) Hoffert, M. I.; Caldeira, K.; Benford, G.; Criswell, D. R.; Green, C.; Herzog, H.; Jain, A. K.; Kheshgi, H. S.; Lackner, K. S.; Lewis, J. S.; Lightfoot, H. D.; Manheimer, W.; Mankins, J. C.; Mauel, M. E.; Perkins, L. J.; Schlesinger, M. E.; Volk, T.; Wigley, T. M. L. *Science* **2002**, *298*, 981.

(36) Vom Stein, T.; Meuresch, M.; Limper, D.; Schmitz, M.; Hölscher, M.; Coetzee, J.; Cole-Hamilton, D. J.; Klankermayer, J.; Leitner, W. *Journal of the American Chemical Society* **2014**, *136*, 13217.